blood®
Regular Article

HEMATOPOIESIS AND STEM CELLS

Extreme disruption of heterochromatin is required for accelerated hematopoietic aging

Christine R. Keenan,[1,2] Nadia Iannarella,[1] Gaetano Naselli,[1] Naiara G. Bediaga,[1,2] Timothy M. Johanson,[1,2] Leonard C. Harrison,[1,2] and Rhys S. Allan[1,2]

[1]The Walter and Eliza Hall Institute of Medical Research, Parkville, VIC, Australia; and [2]Department of Medical Biology, The University of Melbourne, Parkville, VIC, Australia

KEY POINTS

- **Murine hematopoiesis can tolerate major disruptions in heterochromatin structure.**
- **Loss of both *Suv39h* enzymes results in accelerated hematopoietic aging revealing an unexpected role for Suv39h2 in healthy hematopoiesis.**

Loss of heterochromatin has been proposed as a universal mechanism of aging across different species and cell types. However, a comprehensive analysis of hematopoietic changes caused by heterochromatin loss is lacking. Moreover, there is conflict in the literature around the role of the major heterochromatic histone methyltransferase Suv39h1 in the aging process. Here, we use individual and dual deletion of *Suv39h1* and *Suv39h2* enzymes to examine the causal role of heterochromatin loss in hematopoietic cell development. Loss of neither *Suv39h1* nor *Suv39h2* individually had any effect on hematopoietic stem cell function or the development of mature lymphoid or myeloid lineages. However, deletion of both enzymes resulted in characteristic changes associated with aging such as reduced hematopoietic stem cell function, thymic involution and decreased lymphoid output with a skewing toward myeloid development, and increased memory T cells at the expense of naive T cells. These cellular changes were accompanied by molecular changes consistent with aging, including alterations in nuclear shape and increased nucleolar size. Together, our results indicate that the hematopoietic system has a remarkable tolerance for major disruptions in chromatin structure and reveal a role for *Suv39h2* in depositing sufficient H3K9me3 to protect the entire hematopoietic system from changes associated with premature aging. (*Blood*. 2020; 135(23):2049-2058)

Introduction

Aging leads to well-characterized changes in the hematopoietic system such as reduced hematopoietic stem cell (HSC) potential and myeloid skewing at the expense of lymphoid output,[1,2] together resulting in impaired immunity[3] and an increase in hematological diseases.[4] Although these cellular changes are well characterized, their molecular drivers are poorly understood.[5]

Epigenetic changes are considered a "hallmark of aging" across different tissues and species.[6] One such change, the loss of heterochromatin, has been posited to be a unifying mechanism of aging across cell types and species.[7] This theory contends that age-related destabilization of tightly compacted chromatin leads to aberrant gene expression leading to cellular dysfunction. Evidence for this theory comes particularly from studies of the lifespan of model organisms[8,9] and studies using models of premature aging syndromes such as Werner syndrome.[10] However, a comprehensive analysis of hematopoietic changes caused by heterochromatin loss is lacking.

Formation of constitutive heterochromatin is catalyzed by the suppressor of variegation 3-9 homologs *SUV39H1* and *SUV39H2*. These enzymes are responsible for the trimethylation of lysine 9 of histone 3 (H3K9me3) leading to recruitment of heterochromatin 1 (HP1) family of proteins and stable gene silencing. *SUV39H1* expression in HSCs from elderly individuals (>70 years) has previously been shown to be ~50% that of young counterparts (<35 years).[11] Similarly, HSCs from old mice express ~40% less *Suv39h1* and ~40% less H3K9me3 than old mice.[11] Interestingly, the role of *SUV39H1* loss in aging is controversial with some studies suggesting a deleterious role[10,11] and others suggesting a protective role.[12] A role for *SUV39H2* has never been investigated in the hematopoietic system presumably due to the fact its basal expression is much lower than *SUV39H1* in adult tissues except the testis.[13] However, our previous studies show that *SUV39H2* is expressed nearly fourfold higher in activated T lymphocytes, compared with naive cells.[14] Furthermore, T lymphocytes lacking *Suv39h1* show residual H3K9me3 levels, suggesting a role for *Suv39h2* in these cells.[15]

Here, we examined the causal role of heterochromatin loss in hematopoietic cell development. We show that the hematopoietic system can largely tolerate major disruption in chromatin

structure and that loss of both Suv39h1 and Suv39h2 enzymes is required to cause a phenotype consistent with premature aging.

Methods

Mice

Suv39h1 and *Suv39h2* null mice[16] were a generous gift from Thomas Jenuwein (Max Planck Institute, Frieburg). Both of these strains of mice were backcrossed to the C57BL/6 strain (from a mixed background of 129/Sv and C57BL/6J) in order to avoid background effects. After >10 generations of backcrossing, single nucleotide polymorphism analysis revealed that these mice were 99.5% identical to C57BL/6 controls (data not shown), and offspring from both strains were born at mendelian frequencies and developed normally as has been previously published on the mixed background.[16] Crossing these strains together resulted in no viable *Suv39h1* and *Suv39h2* double-knockout (*Suv39h DKO*) mice, with the DKO genotype found to cause embryonic lethality sometime between embryonic day 14 (e14) and e18.

Fetal liver chimeras were generated by harvesting e13 fetal liver cells ($CD45.2^+$) of desired genotype, which were injected into the tail vein (1.5 million per mouse) of lethally irradiated (2× 550 Gy) congenic ($CD45.1^+$) recipient mice. Bone marrow chimeras were generated by harvesting the bone marrow from fetal liver chimeras (8 weeks following reconstitution), which we used to perform secondary reconstitution (5 million per mouse) into new irradiated recipient mice ($CD45.1^+$). Reconstitution was checked at 6 weeks, and all other endpoints were performed at 8 to 12 weeks. In order to perform competitive reconstitution experiments, $CD45.1^+$ bone marrow was harvested from fetal liver chimeras, mixed with equal cell numbers of $CD45.2^+$ bone marrow of desired genotype from fetal liver chimeras, and 5 million cells were injected into a lethally irradiated F1 ($CD45.1^+$/$CD45.2^+$) mouse.

In order to increase the probability of achieving DKO embryos, we used a mating strategy of crossing a Suv39h double heterozygous (*Suv39h1*$^{+/-}$/ *Suv39h2*$^{+/-}$) female with a *Suv39h2* null male (*Suv39h1*$^{+/y}$/ *Suv39h2*$^{-/-}$), which is a mating unable to produce wild-type (WT) embryos. With this mating strategy, DKO embryos were obtained at half-expected mendelian ratios (1/16 obtained compared with 1/8 expected). Embryos WT for *Suv39h1* and heterozygous for *Suv39h2* were therefore used as littermate controls (designated "Control" throughout). Fetal liver chimeras produced from *Suv39h1*-deficient and *Suv39h2*-deficient embryos were matched with true WT littermate controls.

All animal experiments were approved in advance by the Walter and Eliza Hall Institute Animal Ethics Committee and conducted in accordance with published guidelines.

Flow cytometry

Single-cell suspensions were generated from primary and secondary mouse lymphoid organs by mechanical homogenization following by red blood cell lysis (156 mM NH_4Cl, 11.9 mM $NaHCO_3$, 97 μM EDTA). Where required, lineage marker$^-$ $Sca\text{-}1^+$ $cKit^+$ cells (LSKs) were isolated by flow cytometric sorting following immunomagnetic enrichment (anti-CD117; Miltenyi) from bone marrow as previously described.[17] Fluorochrome-conjugated antibodies against the following mouse antigens were then used for analysis and sorting by flow cytometry: CD45.1-eFluor450 (clone A20), Ly6c-eFluor450 (clone HK1.4), TCRβ-PerCPCy5.5 (clone H57-597) from eBioscience; CD4-PECy7 or -PE (clone GK1.5), CD44-APCCy7 (clone IM7), CD150-BV421 (clone 1D4B), CXCR2-A647 (clone SA044G4) from Biolegend; CD62L-PB (clone MEL-14), c-Kit(CD117)-A647 (clone 2B8), Sca-1-A594 (clone E13.161.7), CD8α-PE or -APC (clone 53.6.7), CD11b-AlexaFluor700 (clone M1/70) were generated internally; CD45.2–fluorescein isothiocyanate (FITC) or -BV786 (clone 104), Siglec-F-PE (clone E50-2440), Ly6g-PECy7 (clone1A8), CD19-PECy7 or -BUV395 (clone 1D3) from BD Pharmingen. Surface staining was carried out at 4°C for 30 minutes. Propidium iodide or SYTOX Blue (Thermo Fisher) exclusion was used as live cell indicator, and SPHERO Rainbow Calibration Beads were used to calculate cell counts.

γH2A.X(phospho-S139) (#ab11174; Abcam) staining was performed on fixed (1% formaldehyde, 15 minutes on ice) and permeabilized (BD Perm/Wash solution #554723, 30 minutes on ice) cells. Staining was detected using a goat anti-rabbit immunoglobulin G (IgG)–fluorescein isothiocyanate (#4050-02) antibody from Southern Biotech.

Antibody-stained cells were analyzed using BD FACSCanto II or BD LSRFortessa X-20 and sorted using BD FACSAria III or BD Influx cell sorter.

Immunoblotting

For immunoblotting, whole cell extracts were prepared by lysing cells for 10 minutes at 95°C in 2% sodium dodecyl sulfate, 66 mM Tris buffer at pH 7.0. Samples were then centrifuged at >13 000*g* for 10 minutes, and supernatant was collected. Equivalent cell numbers were resolved in denaturing conditions in 4% to 12% gradient sodium dodecyl sulfate–polyacrylamide gel electrophoresis (Invitrogen) and were transferred onto nitrocellulose membrane (BioRad). Membranes were probed with the following antibodies: rabbit anti-H3K9me3 (#ab8898; Abcam), rabbit anti-Lamin B1 (#ab16048; Abcam), rabbit anti-Histone H3 (#ab1791; Abcam). Densitometry was performed using FIJI/ImageJ software.

Immunofluorescence

Sorted cells were adhered to poly-L-lysine–coated high-performance coverslips (thickness #1.5; Zeiss) and then were fixed in 4% formaldehyde for 10 minutes at room temperature. Fixed cells were permeabilized in 0.2% Triton X-100 for 10 minutes at room temperature; then nonspecific sites were blocked using 5% bovine serum albumin/phosphate-buffered saline for at least 1 hour at room temperature prior to incubation with primary antibodies overnight at 4°C and then were fluorescence-conjugated secondary antibodies for 1.5 hours at room temperature. Coverslips were then mounted in 4′,6-diamidino-2-phenylindole (DAPI)-containing mounting medium and sealed with nail polish. Confocal and Airyscan imaging was then performed on a Zeiss 880 LSM laser scanning microscope using a Plan-Apochromat oil immersion 63× objective with 1.4 numerical aperture. Primary antibodies used were mouse anti-HP1α (#05-689; Millipore), rabbit anti-Lamin B1 (#ab16048; Abcam), and mouse anti-Fibrillarin (#ab4566; Abcam). Secondary antibodies used were goat anti-rabbit IgG AlexaFluor555 (#A21429; Invitrogen) and goat anti-mouse IgG1 AlexaFluor647

(#A21240; Invitrogen). Microscopy analysis was performed using FIJI/ImageJ software using custom-written macros. Colocalization of HP1α fluorescence with DAPI bright regions was determined by initially segmenting individual cell nuclei from a multicell image and then creating a mask for each channel by manual thresholding to define the localization of DAPI bright regions and HP1α fluorescence above background (supplemental Figure 1, available on the *Blood* Web site). The colocalization index was determined independent of the size of surface analyzed by the following formula: $(area_{HP1\alpha} \cap area_{DAPI\text{-}bright})/area_{DAPI\text{-}bright}$. To determine the volume of fibrillarin spots, nuclei were smoothed and filtered using the median 3-dimensional algorithm with x/y/z dimensions set to 2.0/2.0/3.0, respectively. Fibrillarin spots were then identified, and individual spot volume was quantified using the 3-dimensional object counter plug-in.

Human cell isolation

Collection of human blood for research studies was approved by Human Research Ethics Committees of Melbourne Health and Walter and Eliza Hall Institute of Medical Research (application 88/03) and conducted in accordance with the Declaration of Helsinki. This study used 2 individual cord-blood donors and 2 aged donors (69 years old and 74 years old), all male. Human peripheral blood mononuclear cells were purified by Ficoll-Hypaque gradient centrifugation and cryopreserved in liquid N2. Thawed peripheral blood mononuclear cells, ≥92% viable by acridine orange–ethidium bromide staining, were stained with anti-human αβ T-cell receptor (TCR; eBioscience; clone IP26, cat. no. 46-9986-42), anti-human CD4 (BD Pharmingen; clone RPA-T4, cat. no. 555349), anti-human CD45RA (BD Pharmingen; clone 5H9, cat. no. 556626), anti-human CD25 (BD Pharmingen; clone M-A251, cat. no. 557741), anti-human CD14 (BioLegend; clone 63D3, cat. no. 367104), anti-human CD16 (BD Pharmingen; clone 3G8, cat. no. 557758), anti-human HLA-DR (eBioscience; clone L243, cat. no. 48-9952-42), and anti-human CD19 (BioLegend; clone HIB19, cat. no. 302238). Naive $CD8^+$ T cells ($CD14^-CD16^-TCR\alpha\beta^+CD4^-CD45RA^+CD25^-$) were isolated by flow-sorting on a FACSAria (BD Biosciences).

Results

HSC potential is reduced in cells lacking both Suv39h1 and Suv39h2 enzymes

Similar to previous studies on a mixed 129/Sv and C57BL/6J background, deletion of both the Suv39h1 and the Suv39h2 enzymes on a pure C57BL/6 background resulted in embryonic lethality.[16] Therefore, in order to investigate the effect of intrinsic loss of Suv39h1 and/or Suv39h2 in the hematopoietic system, we generated chimeric mice using *Suv39h1*-deficient (h1KO), *Suv39h2*-deficient (h2KO), or double-deficient (DKO) fetal liver cells harvested at e13 (Figure 1A). Donor vs recipient cells were identified by congenic markers (donor: $CD45.2^+$; recipient: $CD45.1^+$). Genetic deletion of Suv39h1 or Suv39h2 individually showed no effect on frequency of $CD45.2^+$ reconstitution compared with WT cells from littermate control embryos; however, deletion of both enzymes resulted in reduced levels of whole blood reconstitution compared with littermate control cells (Figure 1B). Reconstitution of DKO cells was further reduced in most cases upon secondary reconstitution of new recipient mice with bone marrow from these fetal liver chimeras (Figure 1C). Importantly, reduced chimerism appeared to be constant over time with 12-month-old chimeric mice showing similar levels of chimerism as 6-week-old mice from the same litter of irradiation (supplemental Figure 2). Poor reconstitution of recipient mice is an indicator of poor stem cell potential; therefore, we next examined the LSK population, a population enriched for HSCs, in bone marrow from these mice. Although LSK numbers were unaltered in the absence of both Suv39h enzymes, the frequency of long-term HSCs ($CD150^+$ LSKs) was reduced (Figure 1D). This contrasts with physiological aging where HSCs numbers actually increase, although the long-term HSCs decline in frequency within this compartment.[2] In order to exclude variations in irradiation efficiency between individual mice, we performed competitive reconstitution experiments where $CD45.1^+$ WT bone marrow was harvested, mixed with equal cell numbers of control, Suv39h1KO, Suv39h2KO, or DKO $CD45.2^+$ bone marrow, and injected into lethally irradiated F1 ($CD45.1^+/CD45.2^+$) mice (Figure 1E). DKO cells were uniformly out-competed by WT cells, confirming stem and progenitor potential was poor in the absence of both Suv39h methyltransferases (Figure 1F). Importantly, Suv39h1-deficient and Suv39h2-deficient bone marrow performed comparably to WT bone marrow, confirming the stem cell defect requires deletion of both Suv39h enzymes (Figure 1F).

The Suv39h-deficient mature hematopoietic system phenocopies changes associated with aging

We next investigated whether Suv39h deficiency resulted in altered development of mature hematopoietic lineages. Development of $CD4^+$ and $CD8^+$ T cells through double-positive (DP) thymocyte precursors was found to be normal in DKO bone marrow chimeras (Figure 2A). However, thymic involution was apparent in DKO bone marrow chimeras with notably smaller thymic size (Figure 2B) and reduced total thymocyte numbers (Figure 2C) evident compared with control mice or mice lacking 1 Suv39h enzyme.

Examination of mature lymphocyte frequencies in secondary lymphoid organs from DKO chimeras revealed a selective loss of $CD8^+$ T cells compared with stable $CD4^+$ T-cell and B-cell compartments (Figure 2D-E). This selective loss of $CD8^+$ T cells was confirmed with quantification of absolute cell numbers (supplemental Figure 3). In contrast, an increased frequency of total myeloid cells ($CD11b^+$) was observed in DKO chimeras compared with WT chimeras or chimeras lacking individual Suv39h enzymes (Figure 2F). Interestingly, our standard gating strategy to identify individual myeloid cell types failed to detect a discrete population of neutrophils in DKO mice (supplemental Figure 4A); therefore, we next further investigated neutrophil development in these mice using established markers of neutrophil maturation.[18] Gating on $CD45.2^+Lin^-cKit^-CD115^-SiglecF^-CXCR4^-$ cells, mature neutrophils ($Ly6g^+CXCR2^+$) can be distinguished from immature neutrophils ($CXCR2^-$). However, when we applied this gating strategy to DKO chimeras, we found an atypical population of cells expressing the $CXCR2^+$ maturation marker in the absence of Ly6g expression (supplemental Figure 4B). Although this population is lacking the expression of this archetypal neutrophil marker, we speculated that these cells were phenotypically mature neutrophils since Ly6g is dispensable for functional competence.[19] Cytospin preparations of this population showed these cells do indeed morphologically resemble mature neutrophils (supplemental Figure 4C). Quantifying individual myeloid populations, including these $Ly6g^{lo}$

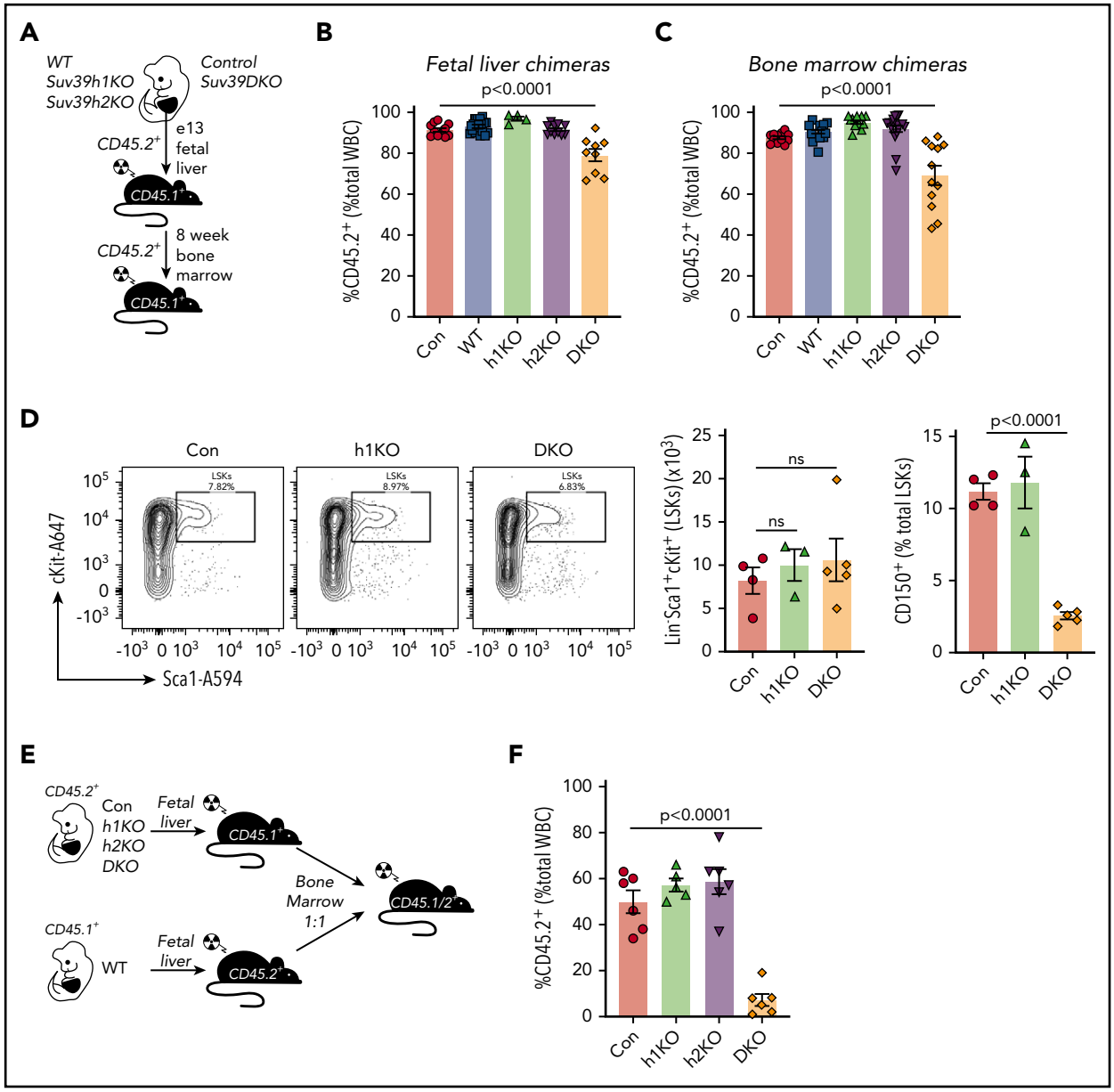

Figure 1. Loss of both Suv39h1 and Suv39h2 enzymes results in poor HSC potential and a reduced frequency of long term HSCs. (A) Schematic of primary and secondary hematopoietic reconstitution of different genotype donor (CD45.2$^+$) cells into lethally irradiated (2× 550 Gy) recipient hosts (CD45.1$^+$). *Suv39h1*-deficient, (h1KO), *Suv39h2*-deficient (h2KO) are matched with littermate WT cells, and double Suv39h-deficient (DKO) are matched with littermate control (Con) cells (*Suv39h2*^{het}). (B-C) Frequency of donor-derived (CD45.2$^+$) total white blood cells (WBC) for each transplanted mouse through 8 weeks in primary (B) and secondary (C) recipients. Individual data points together with mean and standard error of the mean (SEM) are shown. Data were statistically analyzed by 1-way analysis of variance (ANOVA) with Sidak multiple comparisons test comparing each genotype with relevant control. (D) Frequency and number of LSK cells and frequency of long-term HSC enriched (CD150$^+$) cells in bone marrow from Control, h1KO, and DKO chimeras. Individual data points together with mean and SEM are shown. Data were statistically analyzed by 1-way ANOVA with Dunnett post hoc test. (E) Schematic of competitive hematopoietic reconstitution of different genotype donor cells into lethally irradiated (2× 550 Gy) F1 recipient hosts. (F) Frequency of CD45.2$^+$ white blood cells from each competitive chimera depicted in panel D. Data shown as individual data points together with mean and SEM. Data were normalized to the mean of the control group, which was set at 50%, and were statistically analyzed by 1-way ANOVA with Sidak multiple comparisons test comparing each genotype with Control. ns, not significant.

cells as mature neutrophils for DKO mice, revealed that the myeloid skewing mice can be attributed to neutrophil and eosinophil compartments (Figure 2F).

Further examination into mature lymphocyte phenotypes revealed increased frequency of CD44$^+$CD62L$^+$ central memory cells in both CD8$^+$ (Figure 2D,F) and CD4$^+$ (not shown) compartments at the expense of naive cells (CD44$^-$CD62L$^+$) in DKO chimeras, but not in mice lacking 1 Suv39h enzyme. In some DKO chimeras, the frequency of CD44$^+$CD62L$^-$ effector memory cell was also increased; however, this was not consistently observed (Figure 2F).

Heterochromatin is extremely disrupted by the loss of both Suv39 homologs

We next explored why Suv39h DKO chimeras show changes in immune cell frequencies consistent with premature aging, whereas chimeras lacking individual Suv39h enzymes appear

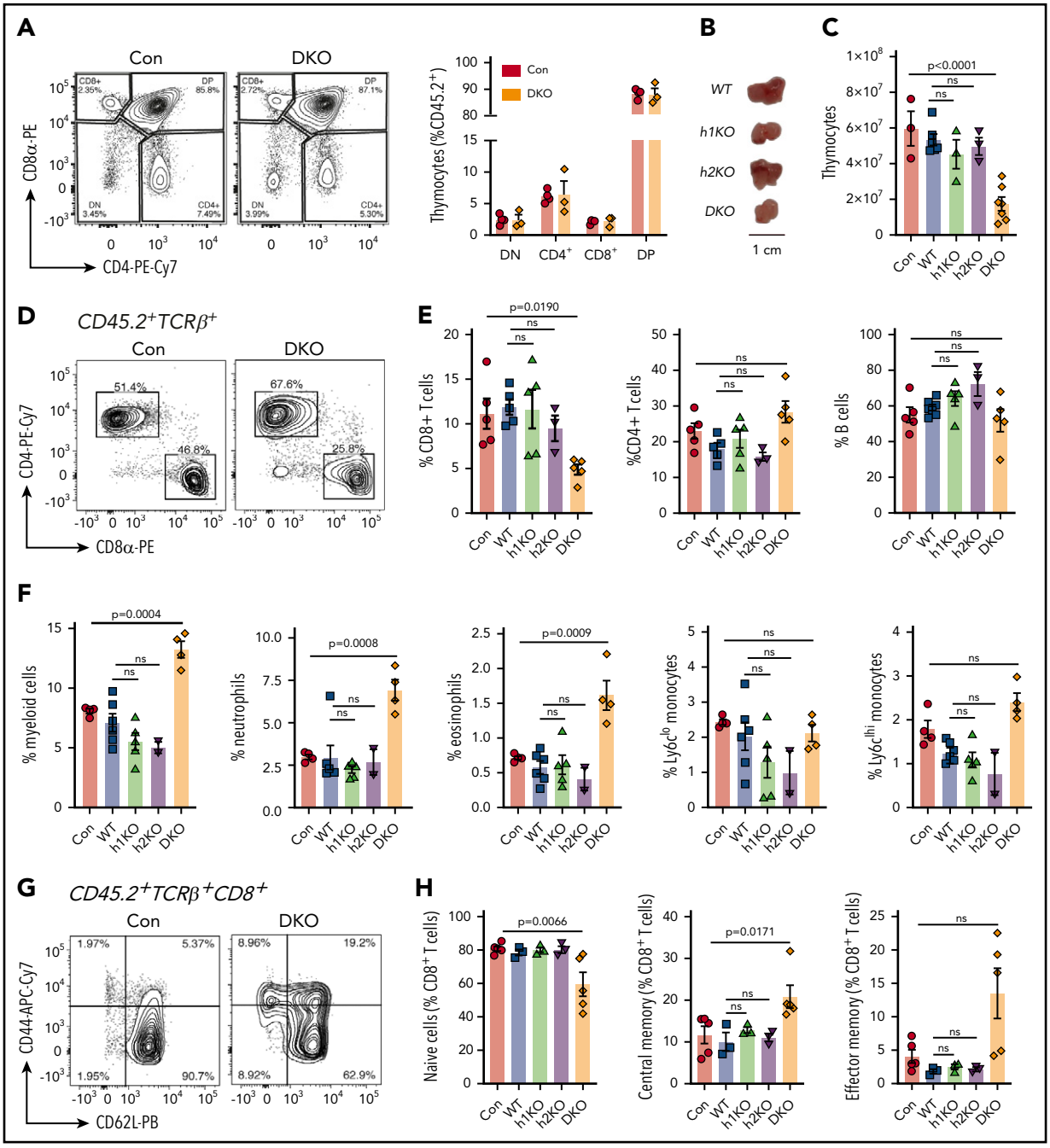

Figure 2. Suv39h DKO results in thymic involution, selective loss of CD8⁺ T cells, myeloid skewing, and increased frequency of memory cells. (A) Frequencies of CD4⁺, CD8⁺, double negative (DN), and DP thymocytes from the thymus of Suv39h1 and h2 DKO and control bone marrow chimeras. (B) Representative images of the dissected thymus from WT, *Suv39h1*-deficient (h1KO), *Suv39h2*-deficient (h2KO), and DKO donor bone marrow chimeras. (C) Total thymocyte numbers obtained from mechanical homogenization and red-cell lysis of thymus tissue from donor cells of different genotypes. (D) Representative flow cytometry plots of T cells (PI⁻CD45.2⁺TCRβ⁺) from peripheral lymph nodes of DKO and control bone marrow chimeras. (E) Splenic frequencies of CD8⁺, CD4⁺ T cells, and B cells (CD19⁺) from bone marrow chimeras of different genotype donor cells. (F) Splenic frequencies of myeloid cells from bone marrow chimeras of different genotype donor cells. Total myeloid cells (CD11b⁺CD11c⁻), neutrophils (CD11b⁺Ly6g⁺Ly6c^{mid}), eosinophils (CD11b⁺SiglecF⁺SSC^{hi}), inflammatory monocytes/macrophages (CD11b⁺Ly6g⁻Ly6c^{Hi}), and resident monocytes/macrophages (CD11b⁺Ly6g⁻Ly6c^{Lo}) are shown. Frequencies of naive (CD62L⁺CD44⁻), central memory (CD62L⁺CD44⁺), and effector memory (CD62L⁻CD44⁺) CD8⁺ T cells from the (G) peripheral lymph nodes and (H) spleens of different donor genotypes. Data in panels C, E, F, and H are depicted as individual data points together with mean and SEM and were statistically analyzed by 1-way ANOVA with Sidak multiple comparisons test comparing each genotype with relevant control.

normal. We began by quantifying global H3K9me3 levels in DP thymocytes as this cell type is highly abundant and the development of DP thymocytes appeared normal in DKO chimeras unlike further differentiated lymphocytes (Figure 2A). As expected, we found H3K9me3 levels to be profoundly reduced in both *Suv39h1*-deficient and DKO cells compared with WT or *Suv39h2*-deficient cells (Figure 3A). However, comparing H3K9me3 levels using increased cell input revealed significantly more residual H3K9me3 levels in cells lacking *Suv39h1* compared with DKO cells (Figure 3B).

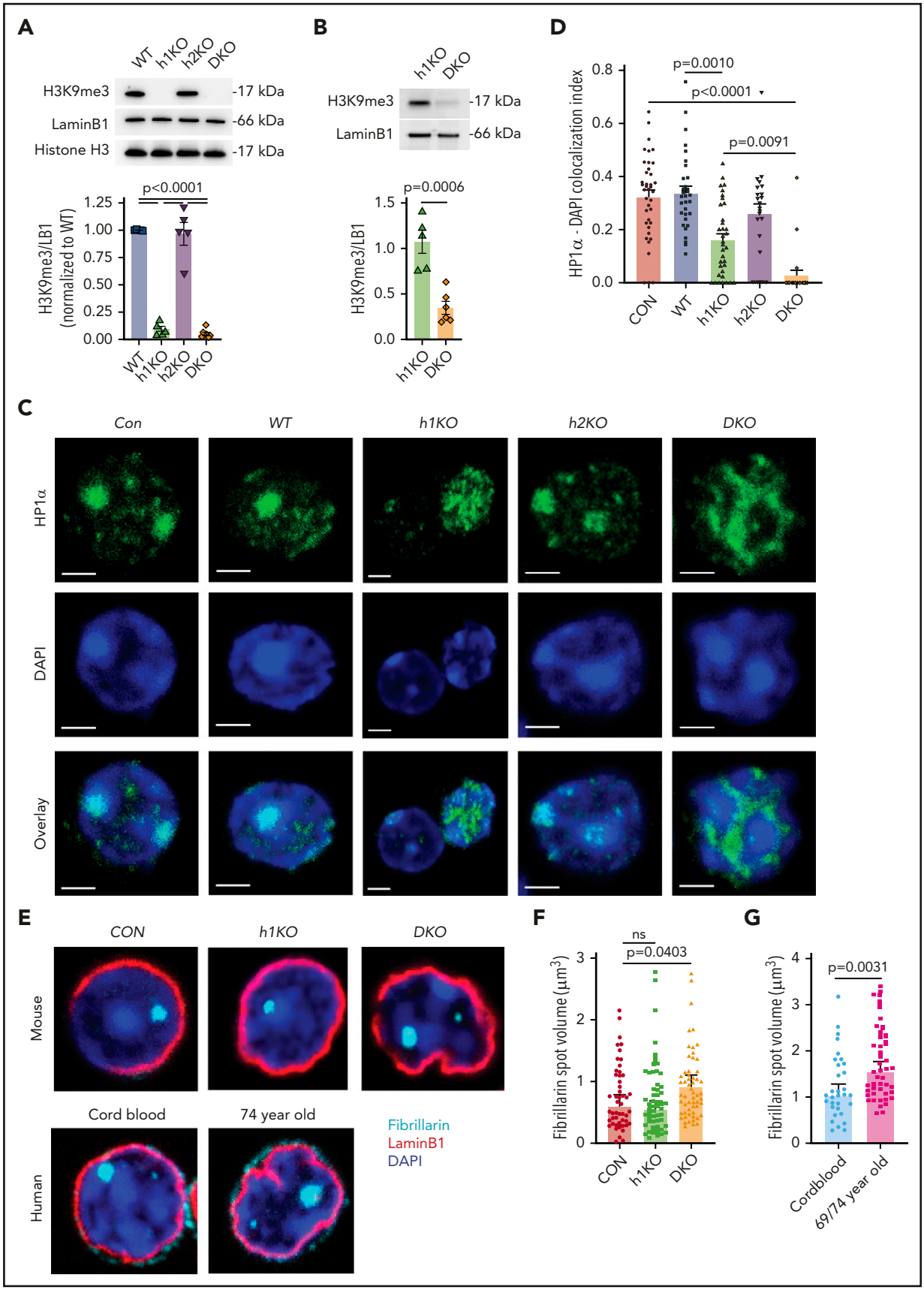

Figure 3. Suv39h DKO lymphocytes show molecular alterations consistent with an aged phenotype. (A) Western blot analysis of H3K9me3 levels from CD45.2^{+} DP thymocytes (50 000 cells loaded per lane) of different genotypes: *Suv39h1*-deficient (h1KO), *Suv39h2*-deficient (h2KO), and DKO. Densitometry data were expressed relative to Lamin B1 (LB1) in that lane and then normalized to WT levels. Mean and SEM together with individual data points are shown. Data were statistically analyzed by 1-way ANOVA

We next examined whether this difference in residual H3K9me3 levels differentially affected heterochromatin structure by performing HP1α immunofluorescence staining. As expected, cell genotypes with high H3K9me3 levels (Con, WT, Suv39h2KO) showed discrete HP1α bright foci in DAPI-bright regions, characteristic of heterochromatin, whereas DKO cells lacking H3K9me3 showed completely relocalized HP1α to DAPI-dim regions usually associated with euchromatin, suggesting loss of heterochromatic structure (Figure 3C). In contrast, Suv39h1-deficient cells showed a mixed phenotype with some cells resembling WT localization, and some cells resembling DKO localization (Figure 3C). Quantification of HP1α colocalization with DAPI bright spots revealed this significant loss of colocalization in the h1KO and near complete loss of colocalization in the DKO thymocytes (Figure 3D). Additional immunofluorescence staining revealed increased nucleolus size in DKO cells compared with control (Figure 3E-F), and distorted nuclear shape compared with round control nuclei or nuclei lacking 1 Suv39h enzyme (Figure 3E). Both these features have been observed in premature aging disorders,[20-22] so we next confirmed these features in physiological aging of hematopoietic cells. By use of peripheral blood $CD8^+$ lymphocytes from aged volunteers as compared with donated cord-blood $CD8^+$ lymphocytes, both increased nucleolus size and distorted nuclear shape are evident (Figure 3E,G).

Given the premature aging phenotype in the Suv39DKO chimeras appeared to begin in the stem cell compartment, we next sorted stem cell–enriched LSK cells from each genotype and performed HP1α localization analysis. Consistent with our data from DP thymocytes, HP1α localization colocalized with DAPI bright regions in WT and Suv39h2-deficient LSK cells, but was markedly disrupted in DKO cells (Figure 4A-B). Suv39h1-deficient LSK cells also showed reduced HP1α localization; however, not to the same extent as we saw in DP thymocytes (Figure 4A-B). We speculate that the extensive rounds of division and differentiation to progress from a bone marrow stem cell through to a DP thymocyte revealed further instability in heterochromatic structure in the Suv39h1KO. The integrity of the nuclear lamina and heterochromatic structure is thought to protect the genome from damage; therefore, we last tested whether genome damage was increased in DKO bone marrow cells by quantifying levels of phospho-γH2AX. We found global phospho-γH2AX levels to be higher in DKO cells, but normal in Suv39h1KO cells, suggesting increased genomic damage in DKO cells with extremely disrupted heterochromatin structure (Figure 4C).

Discussion

Loss of heterochromatin has been posited as a universal theory of aging.[7] However, our data here would suggest that extreme loss of heterochromatin is required to manifest hematopoietic changes archetypal of aging. Importantly, these results reveal a role for Suv39h2 in the adult immune system and suggest that the hematopoietic system can largely tolerate major disruption in chromatin structure.

Our results would suggest that there may be a critical minimum threshold of H3K9me3 in an individual cell nucleus for appropriate heterochromatin formation and maintenance, and secondarily appropriate lamin-association and stability of nuclear structure. The existence of such a threshold is consistent with recent studies describing heterochromatin as a phase-separated compartment.[23,24] Remarkably, Suv39h1-deficient cells show equivalent "fitness" as C57Bl/6 WT cells, despite extensive loss of H3K9me3 and most cells showing disrupted heterochromatin structure as measured by HP1α localization. Interestingly, when we compare quantitative HP1α-DAPI colocalization in DP thymocytes with that observed in LSKs, the Suv39h1KO and DKO cells show greater loss of heterochromatic structure in the DP thymocytes. This could suggest an increased reliance on Suv39 enzymes in more differentiated T cells. Alternatively, instability in heterochromatic structure in the Suv39h1KO may only be revealed following the extensive rounds of division and differentiation to progress from a bone marrow stem cell through to a DP thymocyte. Although we believe this difference in H3K9me3 levels, and resultant effects on heterochromatin structure, is the most likely mechanism discriminating between the premature aging phenotype of DKO compared with Suv39h1-deficient chimeras, we cannot rule out other possible explanations such as a noncanonical function of Suv39h2 such as occurs with other repressive histone methyltransferase enzymes such as enhancer of zeste homolog 2.[25] Our results suggest that loss of H3K9me3 can be quite well tolerated until extremely low levels are reached. This is consistent with recent chromatin immunoprecipitation–sequencing studies in aged human HSCs, which shows a loss of activation-associated histone marks such as H3K4me3 and H3K27ac rather than repressive marks such as H3K27me3,[26] although H3K9me3 was not measured in this study.

SUV39H1 has previously been implicated as both detrimental[10] and protective[12] in premature-aging syndromes. The only study examining SUV39H1 in any hematopoietic lineage observed subtle effects on the myeloid/B lymphoid ratio using cells from Suv39h1-deficient mice on a mixed genetic background.[11] However, here, on a pure C57BL/6 background, *Suv39h1* deficiency alone did not produce noticeable effects on the development of either lymphoid or myeloid lineages in mice. Loss of both Suv39h enzymes remarkably phenocopied the changes associated with physiological aging. We see poor HSC function, a feature well documented in physiological aging.[2,27,28] We also

Figure 3 (continued) with Holm-Sidak multiple comparisons test comparing all genotypes with all others. (B) Western blot analysis of H3K9me3 levels from $CD45.2^+$ DP thymocytes of *Suv39h1*-deficient and *DKO* genotypes (400 000 cells loaded per lane). Mean and SEM together with individual data points are shown. Data were statistically analyzed by Student *t* test. (C) Representative immunofluorescence staining of heterochromatin protein 1-α (HP1α) and colocalization with DAPI bright spots. Scale bar depicts 2 μm. (D) Quantification of colocalization index of thresholded HP1α staining with DAPI bright spots. Data are shown as individual data points together with mean and SEM. Statistical analysis by Kruskal-Wallis *H* test with Dunn post hoc test. n = 40, 32, 35, 31, 30, respectively, pooled from at least 3 mice of each genotype. (E) Representative immunofluorescence staining of Fibrillarin, Lamin B1, and DAPI from $CD45.2^+$ mouse DP thymocytes and human $CD8^+$ T lymphocytes from cord blood and aged (69 and 74 year old) volunteers (representative of 2 donors of each age). Quantification of fibrillarin spot volume (F-G) shows individual nuclei pooled from all samples together with geometric mean and 95% confidence interval. Data in panel F statistically analyzed by Mann-Whitney *U* test. Data in panel G statistically analyzed by Kruskal-Wallis *H* test with Dunn post hoc test. All microscopy images were captured on a Zeiss 880 LSM Laser Scanning Microscope with Airyscan using a 63× Oil Immersion Objective with Numerical Aperture of 1.4.

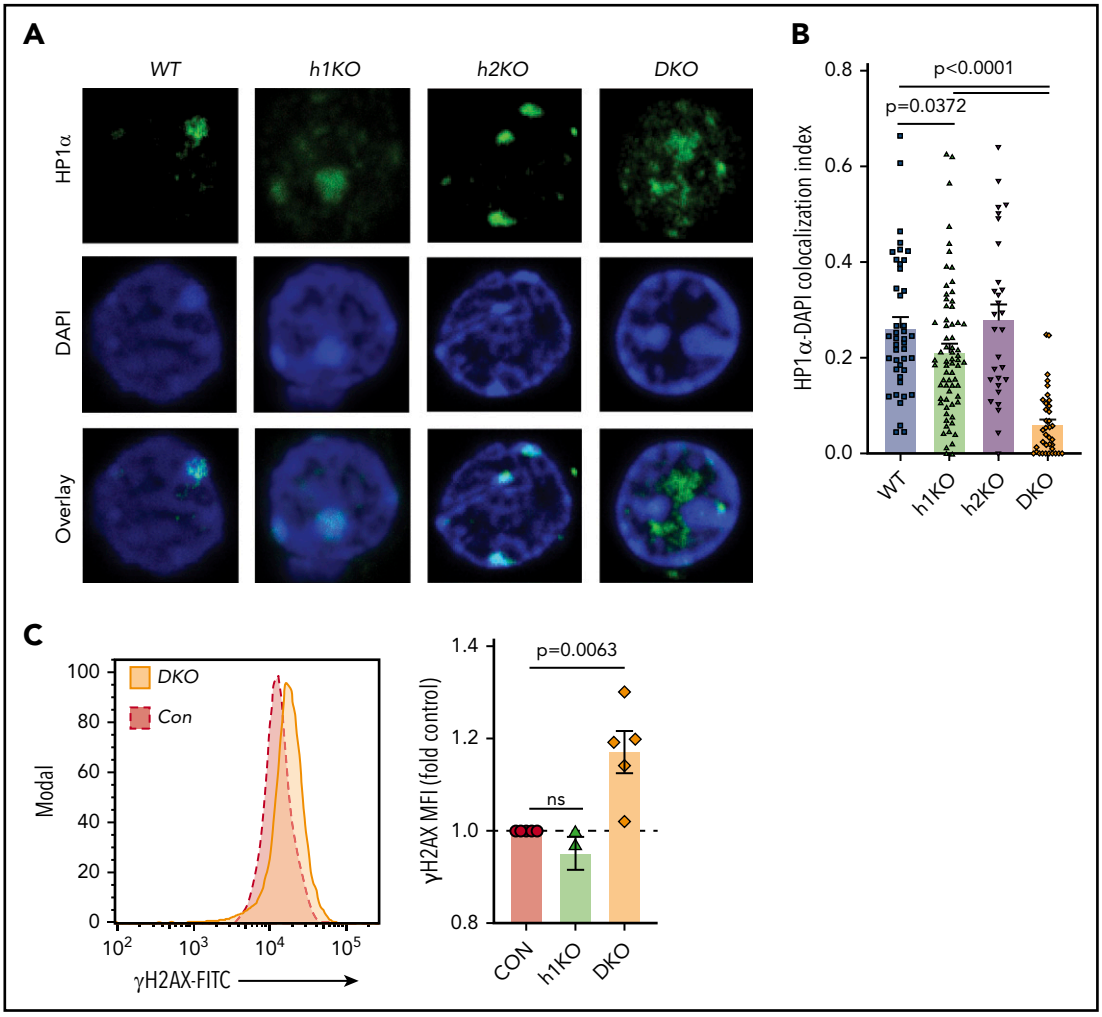

Figure 4. Suv39h DKO stem cells show loss of heterochromatin structure and increased DNA damage. (A) Representative immunofluorescence staining of heterochromatin protein 1-α (HP1α) and colocalization with DAPI bright spots in fluorescence-activated cell sorted LSK cells of different genotypes. Images were captured on a Zeiss 880 LSM Laser Scanning Microscope with Airyscan using a 63× Oil Immersion Objective with Numerical Aperture of 1.4. (B) Quantification of colocalization index of thresholded HP1α staining with DAPI bright spots. Data are shown as individual data points together with mean and SEM. Statistical analysis by 1-way ANOVA with Holm-Sidak post hoc test. n = 42, 68, 30, 37, respectively, pooled from at least 3 mice of each genotype. (C) Phospho-γH2AX staining of bone marrow cells from Suv39h1-deficient (h1KO), Suv39h1- and h2-deficient (*DKO*), and control chimeras. Median fluorescence intensity (MFI) is shown normalized to control levels. Individual data points are shown together with mean and SEM. Data were statistically analyzed by 1-sample Student *t* test (2-tailed) compared with a theoretical mean of 1.0. FITC, fluorescein isothiocyanate.

see myeloid skewing and lymphoid deficits[1,29] in DKO chimeras: in particular, reduced thymic lymphocyte output, a measurable feature of human aging from as young as 1 year old,[30] as well as reductions in peripheral CD8$^+$ T-cell numbers, presumably partly due to the reduced thymic output as well as homeostatic mechanisms in the periphery given CD4$^+$ T cells are not affected. Critically, this selective loss in the CD8$^+$ T-cells compartment phenocopies human physiological aging compared with the relatively stable CD4$^+$ T-cell compartment,[31,32] although the mechanism for this difference is unknown. We also see increased memory cells in *DKO* chimeras, a characteristic of aging in both mice and humans,[33-35] despite being cohoused with control mice. Although reduced B-lymphocyte output is also characteristic of aging,[36,37] we did not see this in our study. We interpret this as a species difference since mouse B-cell numbers are documented to be stable in age (although their function is compromised), unlike human B cells, which decline.[38] Furthermore, physiological aging is associated with increased HSC numbers, although long-term HSCs decline in frequency within this compartment,[2] whereas our DKO chimeras showed unchanged LSK numbers with reduced LT-HSC (CD150$^+$) frequencies. Therefore, the mechanism by which stem-cell function was reduced may be different. Critically, the DKO chimeras phenocopy other age-related hematopoietic changes such as selective reduction in CD8$^+$ T cells and myeloid skewing.

The premature-aging phenotype of the Suv39DKO hematopoietic system contrasts with the effect of inhibiting or deleting other H3K9 methyltransferase enzymes such as Setdb1, another H3K9me3 methyltransferase that has roles in euchromatic regions,[39] unlike the heterochromatic roles of Suv39h enzymes, and G9a/GLP responsible for mono- and dimethylation at H3K9 (H3K9me1/2). Recent studies show that Setdb1 is essential for the maintenance of HSCs and that deletion of Setdb1 using a tamoxifen-inducible *Rosa:Cre-ERT* system leads to a loss of HSCs and a complete failure to repopulate the hematopoietic system, with all Setdb1-deficient mice dying within 21 days of tamoxifen treatment.[40] In contrast, inhibition of G9a/GLP with UNC0638

leads to an accumulation of HSCs in vitro[41,42]; however, hematopoietic reconstitution is not altered by UNC0638 treatment.[42]

Interestingly, complete loss of heterochromatin as seen in Suv39h DKO cells does not just result in cellular changes associated with aging, but it results in other molecular changes. Perhaps it is not surprising that the shape of the nuclear lamina is altered in the absence of the stabilization provided by heterochromatin. However, it is less obvious why increased nucleolar size, and presumably increased ribosomal biogenesis, is observed in DKO cells. One previous study has linked Lamin B1 expression with nucleolar structure and RNA synthesis,[43] revealing a molecular network from the nuclear lamina through to the nucleoli. Our observation of increased nucleolar size could therefore be a biophysical consequence of losing lamina-bound heterochromatin. Alternatively, the poor HSC output might result in an increased requirement for peripheral homeostatic proliferation of descendent lineages, placing these committed cells under greater stress and increased metabolic load. Indeed, HSC dysfunction in physiological aging has been shown to be cell-intrinsic with age-dependent transcriptional alterations predicting downstream developmental potential.[27] This dysfunction could theoretically manifest all the downstream aging-associated cellular changes in physiological aging and the rapid aging of the *Suv39h*-deficient hematopoietic system. Although dysregulated Lamin A/C, the classic driver of the premature aging Hutchinson-Gilford progeria syndrome, causes alterations in nuclear shape of mesenchymal cells,[22] the vast majority of lineages of the hematopoietic system do not express the *LMNA* gene but rather express B-type lamins as the filamentous components of the nuclear lamina. Our results indicate that loss of nuclear structure in DKO cells is not driven by a loss of protein components of the nuclear lamina with Lamin B1 expression stable across genotypes (Figure 4A), but is rather driven by the loss of stabilization provided by the heterochromatin domains themselves. The fact that hematopoietic cells do not express Lamin A/C reinforces the idea that molecular mechanisms cannot be ubiquitously applied to other cell types and systems, but rather must be carefully investigated in the hematopoietic system in order to understand hematopoietic aging.[5]

At this stage, we do not know whether *Suv39h1*-deficient cells would similarly display a premature aging phenotype if left to physiologically age longer. However, our results do allow us to conclude that *Suv39h1*-deficient cells are at least somewhat protected by the expression of *Suv39h2*, not previously thought to have any role in adult tissues other than the testis. Although our results do not disprove the theory of loss of heterochromatin as a universal mechanism of aging across cell types and species,[7] they do indicate that the hematopoietic system has a remarkable tolerance for major disruptions in heterochromatin structure. Furthermore, we reveal a role for *Suv39h2* in depositing sufficient H3K9me3 to protect the entire hematopoietic system from changes associated with premature aging.

Acknowledgments

The authors thank Thomas Jenuwein (MPI, Frieburg) for the Suv39h-deficient mice, Simon Willis (Walter and Eliza Hall Institute) for performing the single nucleotide polymorphism analysis, and Sihara Jayasekera for performing some of the HP1α/DAPI colocalization analyses. The authors acknowledge the tremendous technical assistance from the staff of the core facilities at the Walter and Eliza Hall Institute, particularly the Flow Cytometry facility (WEHIFACS), the Centre for Dynamic Imaging, and the Bioservices department.

This work was supported by grants and fellowships from the National Health and Medical Research Council of Australia, 1125436 (C.R.K.), 1124081 (T.M.J.), 1080887 (L.C.H.), 1100451 (R.S.A.), and the Australian Research Council grant 130100541 (R.S.A.). This study was made possible through Victorian State Government Operational Infrastructure Support and Australian Government NHMRC Independent Research Institute Infrastructure Support scheme and the Australian Cancer Research Fund.

Authorship

Contribution: C.R.K., N.I., and T.M.J. performed the experiments; C.R.K. analyzed the results and wrote the paper; G.N., N.G.B., and L.C.H. provided human materials; and R.S.A. supervised the research and wrote the paper.

Conflict-of-interest disclosure: The authors declare no competing financial interests.

ORCID profiles: C.R.K., 0000-0002-6057-1855; N.G.B., 0000-0002-7363-0068; R.S.A., 0000-0003-0906-2980.

Correspondence: Christine R. Keenan, Immunology Division, Walter and Eliza Hall Institute of Medical Research, 1G Royal Parade, Parkville, VIC 3052, Australia; e-mail: keenan.c@wehi.edu.au; and Rhys S. Allan, Immunology Division, Walter and Eliza Hall Institute of Medical Research, 1G Royal Parade, Parkville, VIC 3052, Australia; e-mail: rallan@wehi.edu.au.

Footnotes

Submitted 22 August 2019; accepted 22 March 2020; prepublished online on *Blood* First Edition 17 April 2020. DOI 10.1182/blood.2019002990.

For original data please contact the corresponding authors.

The online version of this article contains a data supplement.

The publication costs of this article were defrayed in part by page charge payment. Therefore, and solely to indicate this fact, this article is hereby marked "advertisement" in accordance with 18 USC section 1734.

REFERENCES

1. Pang WW, Price EA, Sahoo D, et al. Human bone marrow hematopoietic stem cells are increased in frequency and myeloid-biased with age. *Proc Natl Acad Sci USA*. 2011; 108(50):20012-20017.

2. Bernitz JM, Kim HS, MacArthur B, Sieburg H, Moore K. Hematopoietic stem cells count and remember self-renewal divisions. *Cell*. 2016; 167(5):1296-1309.e1210.

3. Kline KA, Bowdish DM. Infection in an aging population. *Curr Opin Microbiol*. 2016;29:63-67.

4. de Haan G, Lazare SS. Aging of hematopoietic stem cells. *Blood*. 2018;131(5):479-487.

5. Keenan CR, Allan RS. Epigenomic drivers of immune dysfunction in aging. *Aging Cell*. 2019;18(1):e12878.

6. López-Otín C, Blasco MA, Partridge L, Serrano M, Kroemer G. The hallmarks of aging. *Cell*. 2013;153(6):1194-1217.

7. Tsurumi A, Li WX. Global heterochromatin loss: a unifying theory of aging? *Epigenetics*. 2012;7(7):680-688.

8. Larson K, Yan SJ, Tsurumi A, et al. Heterochromatin formation promotes longevity and represses ribosomal RNA synthesis. *PLoS Genet*. 2012;8(1):e1002473.

9. Siebold AP, Banerjee R, Tie F, Kiss DL, Moskowitz J, Harte PJ. Polycomb Repressive Complex 2 and Trithorax modulate

Drosophila longevity and stress resistance. *Proc Natl Acad Sci USA*. 2010;107(1):169-174.

10. Zhang W, Li J, Suzuki K, et al. Aging stem cells. A Werner syndrome stem cell model unveils heterochromatin alterations as a driver of human aging. *Science*. 2015;348(6239): 1160-1163.

11. Djeghloul D, Kuranda K, Kuzniak I, et al. Age-associated decrease of the histone methyltransferase SUV39H1 in HSC perturbs heterochromatin and B lymphoid differentiation. *Stem Cell Reports*. 2016;6(6):970-984.

12. Liu B, Wang Z, Zhang L, Ghosh S, Zheng H, Zhou Z. Depleting the methyltransferase Suv39h1 improves DNA repair and extends lifespan in a progeria mouse model. *Nat Commun*. 2013;4(1):1868.

13. O'Carroll D, Scherthan H, Peters AH, et al. Isolation and characterization of Suv39h2, a second histone H3 methyltransferase gene that displays testis-specific expression. *Mol Cell Biol*. 2000;20(24):9423-9433.

14. Keenan CR, Iannarella N, Garnham AL, et al. Polycomb repressive complex 2 is a critical mediator of allergic inflammation. *JCI Insight*. 2019;4(10):e127745.

15. Allan RS, Zueva E, Cammas F, et al. An epigenetic silencing pathway controlling T helper 2 cell lineage commitment. *Nature*. 2012; 487(7406):249-253.

16. Peters AH, O'Carroll D, Scherthan H, et al. Loss of the Suv39h histone methyltransferases impairs mammalian heterochromatin and genome stability. *Cell*. 2001;107(3):323-337.

17. Johanson TM, Lun ATL, Coughlan HD, et al. Transcription-factor-mediated supervision of global genome architecture maintains B cell identity. *Nat Immunol*. 2018;19(11): 1257-1264.

18. Evrard M, Kwok IWH, Chong SZ, et al. Developmental analysis of bone marrow neutrophils reveals populations specialized in expansion, trafficking, and effector functions. *Immunity*. 2018;48(2):364-379.e368.

19. Hasenberg A, Hasenberg M, Männ L, et al. Catchup: a mouse model for imaging-based tracking and modulation of neutrophil granulocytes. *Nat Methods*. 2015;12(5):445-452.

20. Buchwalter A, Hetzer MW. Nucleolar expansion and elevated protein translation in premature aging. *Nat Commun*. 2017;8(1):328.

21. Goldman RD, Shumaker DK, Erdos MR, et al. Accumulation of mutant lamin A causes progressive changes in nuclear architecture in Hutchinson-Gilford progeria syndrome. *Proc Natl Acad Sci USA*. 2004;101(24):8963-8968.

22. Scaffidi P, Misteli T. Lamin A-dependent nuclear defects in human aging. *Science*. 2006; 312(5776):1059-1063.

23. Strom AR, Emelyanov AV, Mir M, Fyodorov DV, Darzacq X, Karpen GH. Phase separation drives heterochromatin domain formation. *Nature*. 2017;547(7662):241-245.

24. Larson AG, Elnatan D, Keenen MM, et al. Liquid droplet formation by HP1α suggests a role for phase separation in heterochromatin. *Nature*. 2017;547(7662):236-240.

25. Nutt SL, Keenan C, Chopin M, Allan RS. EZH2 function in immune cell development [published online ahead of print 28 February 2020]. *Biol Chem*. 202019.

26. Adelman ER, Huang HT, Roisman A, et al. Aging human hematopoietic stem cells manifest profound epigenetic reprogramming of enhancers that may predispose to leukemia. *Cancer Discov*. 2019;9(8):1080-1101.

27. Rossi DJ, Bryder D, Zahn JM, et al. Cell intrinsic alterations underlie hematopoietic stem cell aging. *Proc Natl Acad Sci USA*. 2005; 102(26):9194-9199.

28. Wahlestedt M, Norddahl GL, Sten G, et al. An epigenetic component of hematopoietic stem cell aging amenable to reprogramming into a young state. *Blood*. 2013;121(21):4257-4264.

29. Dykstra B, Olthof S, Schreuder J, Ritsema M, de Haan G. Clonal analysis reveals multiple functional defects of aged murine hematopoietic stem cells. *J Exp Med*. 2011;208(13): 2691-2703.

30. Palmer S, Albergante L, Blackburn CC, Newman TJ. Thymic involution and rising disease incidence with age. *Proc Natl Acad Sci USA*. 2018;115(8):1883-1888.

31. Briceño O, Lissina A, Wanke K, et al. Reduced naïve CD8(+) T-cell priming efficacy in elderly adults. *Aging Cell*. 2016;15(1):14-21.

32. Wertheimer AM, Bennett MS, Park B, et al. Aging and cytomegalovirus infection differentially and jointly affect distinct circulating T cell subsets in humans. *J Immunol*. 2014; 192(5):2143-2155.

33. Nikolich-Žugich J. Aging of the T cell compartment in mice and humans: from no naive expectations to foggy memories. *J Immunol*. 2014;193(6):2622-2629.

34. Quinn KM, Fox A, Harland KL, et al. Age-related decline in primary $CD8^+$ T cell responses is associated with the development of senescence in virtual memory $CD8^+$ T cells. *Cell Rep*. 2018;23(12):3512-3524.

35. Su LF, Kidd BA, Han A, Kotzin JJ, Davis MM. Virus-specific CD4(+) memory-phenotype T cells are abundant in unexposed adults. *Immunity*. 2013;38(2):373-383.

36. Dorshkind K, Montecino-Rodriguez E, Signer RA. The ageing immune system: is it ever too old to become young again? *Nat Rev Immunol*. 2009;9(1):57-62.

37. Ogawa T, Kitagawa M, Hirokawa K. Age-related changes of human bone marrow: a histometric estimation of proliferative cells, apoptotic cells, T cells, B cells and macrophages. *Mech Ageing Dev*. 2000;117(1-3): 57-68.

38. Frasca D, Landin AM, Riley RL, Blomberg BB. Mechanisms for decreased function of B cells in aged mice and humans. *J Immunol*. 2008; 180(5):2741-2746.

39. Dodge JE, Kang YK, Beppu H, Lei H, Li E. Histone H3-K9 methyltransferase ESET is essential for early development. *Mol Cell Biol*. 2004;24(6):2478-2486.

40. Koide S, Oshima M, Takubo K, et al. Setdb1 maintains hematopoietic stem and progenitor cells by restricting the ectopic activation of nonhematopoietic genes. *Blood*. 2016;128(5): 638-649.

41. Chen X, Skutt-Kakaria K, Davison J, et al. G9a/GLP-dependent histone H3K9me2 patterning during human hematopoietic stem cell lineage commitment. *Genes Dev*. 2012;26(22): 2499-2511.

42. Ugarte F, Sousae R, Cinquin B, et al. Progressive chromatin condensation and H3K9 methylation regulate the differentiation of embryonic and hematopoietic stem cells. *Stem Cell Reports*. 2015;5(5):728-740.

43. Martin C, Chen S, Maya-Mendoza A, Lovric J, Sims PF, Jackson DA. Lamin B1 maintains the functional plasticity of nucleoli. *J Cell Sci*. 2009;122(Pt 10):1551-1562.